axioms

MDPI

Communication

Hydraulic Losses in Systems of Conduits with Flow from Laminar to Fully Turbulent: A New Symbolic Regression Formulation

Marko Milošević [1], Dejan Brkić [1,*], Pavel Praks [2], Dragan Litričin [3] and Zoran Stajić [1]

[1] Faculty of Electronic Engineering, University of Niš, 18000 Niš, Serbia; marko.milosevic@elfak.ni.ac.rs (M.M.); zoran.stajic@elfak.ni.ac.rs (Z.S.)
[2] IT4Innovations, VSB–Technical University of Ostrava, 708 00 Ostrava, Czech Republic; pavel.praks@vsb.cz
[3] Siemens, Siemensova 1, 155 00 Prague, Czech Republic; dragan.litricin@siemens.com
* Correspondence: dejanbrkic0611@gmail.com or dejan.brkic@elfak.ni.ac.rs

Abstract: Separate flow friction formulations for laminar and turbulent regimes of flow through pipes are in common use in engineering practice. However, variation of different parameters in a system of conduits during conveying of fluids can cause changes in flow pattern from laminar to fully turbulent and vice versa. Because of that, it is useful to unify formulations for laminar and turbulent hydraulic regimes in one single coherent equation. In addition to a physical interpretation of hydraulic friction, this communication gives a short overview of already available Darcy's flow friction formulations for both laminar and turbulent flow and additionally includes two simple completely new approximations based on symbolic regression.

Keywords: pipeline design; hydraulic friction; Colebrook equation; Moody chart; Reynolds number; relative roughness; pressure loss; laminar flow; turbulent flow; symbolic regression

MSC: 62J02; 68W30; 68T20; 74P10; 76N25

Citation: Milošević, M.; Brkić, D.; Praks, P.; Litričin, D.; Stajić, Z. Hydraulic Losses in Systems of Conduits with Flow from Laminar to Fully Turbulent: A New Symbolic Regression Formulation. *Axioms* **2022**, *11*, 198. https://doi.org/10.3390/axioms11050198

Academic Editor: Gabriella Bretti

Received: 6 March 2022
Accepted: 20 April 2022
Published: 24 April 2022

1. Introduction

To avoid the inconvenience of determining which type of hydraulic regimes occurs in pipes, a coherent equation that unifies laminar and turbulent flow friction would be useful [1–3]. This Communication gives a short overview of a few already existing such formulations and also includes two completely new approximations which are generated using symbolic regression [4] and which efficiently can approximate flow friction during both laminar and turbulent flow through pipes. Coherent formulas which unify laminar and turbulent flow should be used in systems of pipes that can be found in offshore oil fields [5,6] or in similar conditions where flow conditions can be changed caused by variations in viscosity due to variation in temperature [7], etc.

This introduction is followed by a short physical interpretation of hydraulic friction, and with an overview of unified equations for laminar and turbulent Darcy's flow friction, which includes two new formulations based on symbolic regression, and, finally, this Communication ends with conclusions. The findings are valid for the Darcy–Weisbach flow model [8,9]. The software tool for testing all presented equations is written in Python and is given in the Supplementary Materials attached to this Communication.

2. Hydraulic Friction

Hydraulic friction is essentially caused due to energy consumption by the interaction between the flowing fluid and the conduit that it is moving through. This loss of energy is mainly manifested through the fall of pressure, which is different in a laminar and turbulent flow. In addition, a short description of already existing works and approaches that gives unified formulas for laminar and turbulent flow is given in this section.

2.1. Physical Interpretation

For the calculation of flow parameters for the transport of fluids through a system of conduits, it is essential to obtain an equation to relate flow and pressure loss. For that, the most used is the empirical Darcy–Weisbach model [10] as given in Equation (1) where one of the most important parameters is Darcy's flow friction λ, which is the main topic of computation in this Communication:

$$\frac{\Delta p}{L} \approx \frac{8 \cdot \lambda \cdot \rho \cdot Q^2}{D^5 \cdot \pi^2} \tag{1}$$

The following symbols are used in Equation (1):

- Δp is pressure loss in Pa;
- L is the length of pipe in m;
- λ is non-dimensional Darcy's flow friction;
- ρ is density of the fluid in kg/m^3;
- Q is flow in m^3/s;
- D is the hydraulic diameter of the pipe in m; and
- π is Ludolph number; $\pi \approx 3.1415$.

In engineering practice, commonly, the non-dimensional Darcy's flow friction λ is calculated using separate formulas for laminar and for turbulent flow:

1. For laminar flow using theoretically founded Hagen–Poiseuille formulation as given in Equation (2):

$$\lambda = \frac{64}{Re} \tag{2}$$

2. For turbulent flow, many empirical formulations are available, but among the most used is given by Colebrook in 1939 [11] in Equation (3), which is empirically based on an experiment with the flow of air through pipes with different inner roughness performed by Colebrook and White in 1937 [12] (while examples of other empirical equations can follow Nikuradse's inflectional shape of curves which modify monotonic behaviour of Colebrook's curves [13,14] or can be based on some newer experiments [15–17]):

$$\frac{1}{\sqrt{\lambda}} \approx -0.8686 \cdot ln\left(\frac{2.51}{Re} \cdot \frac{1}{\sqrt{\lambda}} + \frac{\varepsilon}{3.71}\right) \tag{3}$$

In Equations (2) and (3), the following symbols are used:

- ln is a natural logarithm;
- λ is non-dimensional Darcy's flow friction;
- $Re \approx V \cdot D/\nu$ is the non-dimensional Reynolds number (V is the flow velocity of the fluid in m/s, D is the hydraulic diameter of the pipe in m, and ν is kinematic viscosity in m^2/s), and
- ε is the non-dimensional relative roughness of the inner pipe surface (if the real absolute roughness of the pipe is $\varepsilon*$, then $\varepsilon = \varepsilon * / D$).

As can be seen from the structure of Equations (2) and (3), flow friction λ in laminar flow depends only on the Reynolds number Re, while, in turbulent flow, effects of the roughness of inner surface ε of the conveying conduits gradually also begin to affect the flow friction λ. The turbulent regime includes smooth, transitional turbulent and rough hydraulic regimes. In more detail, in laminar and smooth turbulent flow regimes, flow friction λ depends only on the Reynolds number Re, for transitional turbulent flow on both the Reynolds number Re and the relative roughness of inner pipe surface ε, while, for a turbulent rough regime, only on the relative roughness of inner pipe surface ε. The value of the inner roughness of pipe depends on the type of material and its condition and age [18–21], and it affects flow by forming a viscous sublayer near the inner pipe wall [22].

A detailed graph for all types of flow, which includes laminar and turbulent regimes, is given by Moody in his diagram [23–25], as given in Figure 1. The turbulent flow of Moody's diagram as given in Figure 1 is based on the Colebrook equation (on the other hand, a similar diagram that follows Nikuradse's findings [13] is given by McGovern [26]).

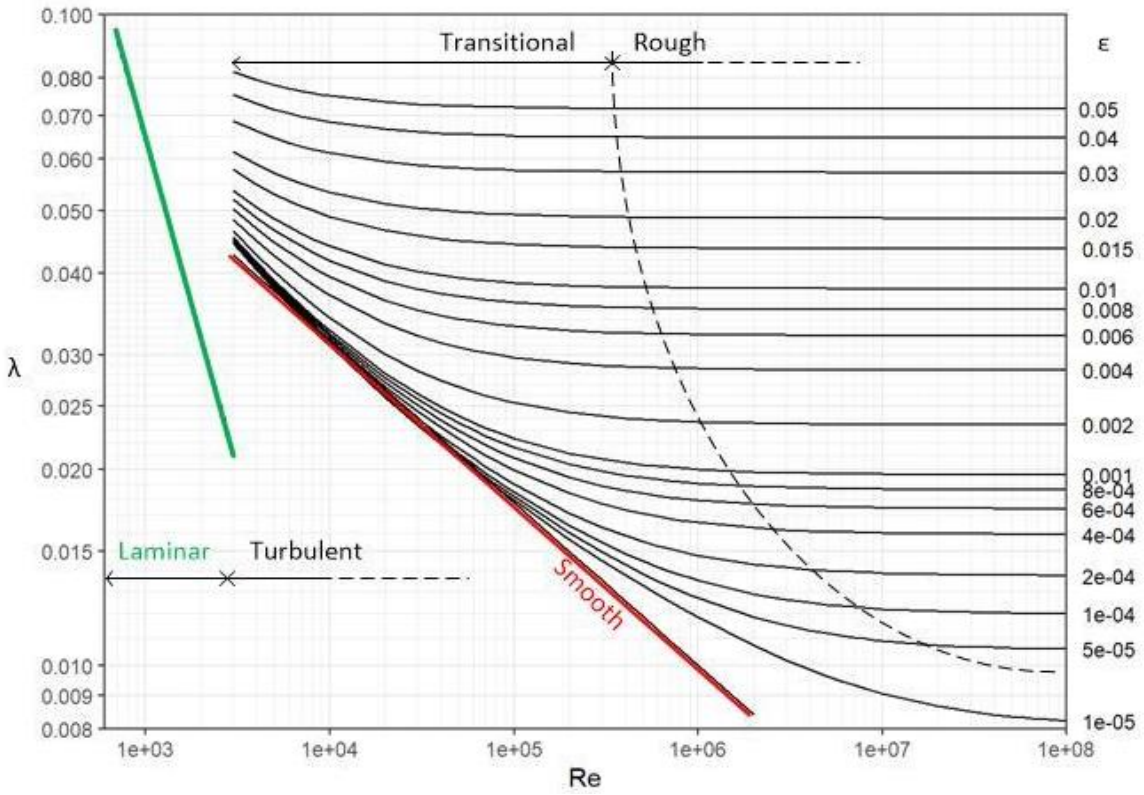

Figure 1. Different flow regimes; Laminar and Turbulent (Turbulent includes Smooth, Transitional and Rough).

Generally, as can be seen in Figure 1, laminar flow occurs for the Reynolds number Re below 2000 or slightly more, then an unstable transition from laminar to turbulent flow occurs between 2000 and 3000–4000, where turbulent regime starts for the Reynolds number Re higher than 4000. In more detail [22,27], a smooth turbulent regime occurs for $\zeta < 16$ while the rough turbulent regime is for $\zeta > 200$, while in between is the transitional turbulent regime, where ζ is defined in Equation (4):

$$\zeta = \varepsilon \cdot Re \cdot \sqrt{\lambda} \tag{4}$$

In Equation (4), the following symbols are used:

- ζ is a non-dimensional parameter that is used for determining the specific type of turbulent flow (in the case of turbulent regime, smooth turbulent flow occurs for $\zeta < 16$, transitional or partial turbulent flow for $16 < \zeta < 200$, while fully developed rough turbulent flow occurs for $\zeta > 200$);
- ε is the non-dimensional roughness of the inner pipe surface (it has no effect on laminar and smooth turbulent flow, partial effect on transitional turbulent flow, and significant effect on fully developed rough turbulent flow);
- Re is the non-dimensional Reynolds number (the flow for $Re < 2320$ is surely laminar);
- λ is the non-dimensional Darcy's hydraulic flow friction factor.

2.2. Background and Related Works

The most difficult part for modelling of the laminar and turbulent part in the sharp change of behaviour between these two regimes. Different approaches are used for modelling this inconvenient circumstance:

1. The main strength of the model from [28,29] is in assuming the sharp flow transition as a sigmoid type of function that results from the randomness of the flow associated with the turbulence;
2. Using balance between mass and energy in the transition from laminar to turbulent flow, Ref. [30] is developed using the formulation for turbulent flow [31], where it is flexible and can be replaced by any other available equation developed for turbulent flow [32–36];
3. Using the rationale that flow friction changes during the flow of oil in offshore pipelines due to variation of viscosity due to temperature oscillations [37], a unified equation from [38] is derived using the equation for turbulent flow [39];
4. The same rationale for the flow of oil, but using experiences from Russian pipelines, a unified equation from [40] is developed on a very common equation from [41], which is in common use in Russian engineering practice for the calculation of turbulent flow friction;
5. The interpolation method which is based on probability is used in [42] to develop a unified model;
6. Through the similar reasoning like for the submarine model, a unified model [43] is developed using a specific equation for turbulent flow from [44] this time;
7. The interchangeable model for unified equation in [45] is based on an experiment from [46] where switching functions between specific flow regimes are developed using symbolic regression, and finally
8. Two unified equations for flow from laminar to turbulent ape developed using symbolic regression, and they are new in this Communication.

The models are presented in the next section of this Communication.

3. Unified Equations for Laminar and Turbulent Darcy's Flow Friction

Although following the same principle to unite laminar and turbulent flow friction λ, some of the equations presented in this section follow Colebrook's monotonic while others Nikuradse's inflectional behaviour for the turbulent flow [27].

The non-dimensional Reynolds number Re together with the non-dimensional relative roughness of inner pipe surface ε are used as inputs in unified flow friction models given in this section, while the non-dimensional Darcy's flow friction λ is valid for both laminar and turbulent flow is an output. All other quantities, such as, in order of their appearance L, T_t, T_f, λ_t, δ, A_1, A_2, A_3, a, b, α, β, x, y, z, T_s, T, are auxiliary in the presented models, while ln is a natural logarithm, log_{10} is decimal logarithm and e is exponential function.

3.1. Six Parameter Model

A six-parameter model to estimate the friction factor λ is given by Díaz-Damacillo and Plascencia [28] and by Plascencia et al. [29]. It follows Nikuradse's inflectional behaviour for its turbulent part. This model is given in Equation (5):

$$\left.\begin{array}{c} \lambda \approx L + T_t + T_f \\ A = \frac{0.77505}{\varepsilon^2} - \frac{10.984}{\varepsilon} + 7953.8 \\ B = \left|0.02 - \left(-2 \cdot \log_{10}\left(\frac{\varepsilon}{3.71}\right)\right)^{-2}\right| \\ L = \frac{64}{Re} \\ T_t = \frac{0.02}{1+e^{\frac{3000-Re}{100}}} \\ T_f = \frac{B}{1+e^{\frac{\varepsilon \cdot (A-Re)}{150}}} \end{array}\right\} \quad (5)$$

3.2. Unified Model Based on the Turbulent Transitional Formula

The structure of the new explicit friction factor formula for laminar and turbulent flow friction given in Equation (6) is developed by Avci and Karagoz [30]. In their paper [30], Avci and Karagoz used a model from their previous work [31] to calculate λ_t, while Equation (6) is modified here with a more accurate formula for turbulent flow friction factor λ_t from Praks and Brkić [32]. The main strength of this formula is that it can be modified using any of many available formulas for turbulent flow friction factor λ_t which can be found for example in [33–36]:

$$\left.\begin{array}{c} \lambda \approx \lambda_t + \left(\frac{64}{Re} - \lambda_t\right) \cdot e^{-\left(\frac{\delta \cdot Re}{2560}\right)^8} \\ \delta = 1 + \varepsilon + \frac{\varepsilon \cdot \sqrt{\varepsilon}}{1 + 225 \cdot \varepsilon^3} + 500 \cdot \varepsilon^4 \\ \lambda_t \approx \left(0.8685972 \cdot \left(A_1 - A_3 + \frac{A_3}{A_2 - 0.5588 \cdot A_3 + 1.2079}\right)\right)^{-2} \\ A_1 = \ln(Re) - 0.779626 \\ A_2 = A_1 + \frac{Re \cdot \varepsilon}{8.0897} \\ A_3 = \ln(A_2) \end{array}\right\} \quad (6)$$

3.3. Submarine Model

Due to variations in the temperature of crude oil, its viscosity also varies [37]. Because of that flow regime, in some parts of the pipeline, it can be turbulent, while, in some other parts, it can be laminar. This can especially occur in submarine pipelines used for transport from offshore locations. Using this reasoning, Swamee [5] (also presented in [38]) developed his formula; Equation (7) is based on his previous work with Jain on the turbulent flow [39]:

$$\lambda \approx \left(\left(\frac{64}{Re}\right)^8 + 9.5 \cdot \left(\ln\left(\frac{\varepsilon}{3.7} + \frac{5.74}{Re^{0.9}}\right) - \left(\frac{2500}{Re}\right)^6\right)^{-16}\right)^{0.125} \quad (7)$$

3.4. Russian Formula for Transport of Crude Oil

Following the same idea for the transport of crude oil through pipelines, Chernikin and Chernikin [40] developed Equation (8), which is based on the equation by Altshul [41] for turbulent flow from Russian practice, which is commonly used there instead of the Colebrook equation:

$$\left.\begin{array}{c} \lambda \approx 0.11 \cdot \left(\frac{a + \varepsilon + b^{1.4}}{115 \cdot b + 1}\right)^{0.25} \\ a = \frac{68}{Re} \\ b = (28 \cdot a)^{10} \end{array}\right\} \quad (8)$$

3.5. Interpolation Method

Cheng [42] used an interpolation method to provide a transition between different flow regimes. Cheng's formula is given in Equation (9). This formula follows data from Nikuradse's experiment [13]:

$$\left.\begin{array}{c} \frac{1}{\lambda} \approx \left(\frac{Re}{64}\right)^{\alpha} \cdot \left(1.8 \cdot \log_{10}\left(\frac{Re}{6.8}\right)\right)^{2 \cdot \beta \cdot (1-\alpha)} \cdot \left(2 \cdot \log_{10}\left(\frac{3.7}{\varepsilon}\right)\right)^{2 \cdot (1-\alpha) \cdot (1-\beta)} \\ \alpha = \frac{1}{1 + \left(\frac{Re}{2720}\right)^9} \\ \beta = \frac{1}{1 + \left(\frac{160}{\varepsilon}\right)^2} \end{array}\right\} \quad (9)$$

3.6. Churchill Equation

The friction-factor equation spanning all fluid-flow regimes by Churchill [43] is given in Equation (10). Churchill's equation is based on his previous formula developed only for turbulent flow [44]:

$$\lambda = 8 \cdot \sqrt[12]{\left(\frac{8}{Re}\right)^{12} + \left[\left(-2.457 \cdot \ln\left(\left(\frac{7}{Re}\right)^{0.9} + 0.27 \cdot \varepsilon\right)\right)^{16} + \left(\frac{37530}{Re}\right)^{16}\right]^{-1.5}} \tag{10}$$

3.7. Multisegmented Equation

The multisegmented equation by Brkić and Praks [45] is developed using the idea by Uršič and Kompare [46] to use any available equation for laminar, turbulent smooth, and turbulent rough hydraulic regimes which are connected using switching functions developed using symbolic regression. One example of this approach is given in Equation (11). All multisegmented equations, no matter the particular equation which is used for segments, follow Nikuradse's inflectional behaviour [13]:

$$\left.\begin{aligned} \lambda &= (1-x)\cdot\tfrac{64}{Re} + (x-z)\cdot T_s + y\cdot T \\ x &= 1 - \frac{1048}{\frac{4.489}{10^{20}}\cdot Re^6\cdot\left(0.148\cdot Re - \frac{2.306\cdot Re}{0.003133\cdot Re + 9.646}\right) + 1050} \\ y &= 1.012 - \frac{1}{0.02521\cdot Re\cdot\varepsilon + 2.202} \\ z &= 1 - \frac{1}{0.000389\cdot Re^2\cdot\varepsilon^2 + 0.0000239\cdot Re + 1.61} \\ T_s &= \tfrac{0.316}{Re^{0.25}} \\ T &= \left(-2\cdot\log_{10}\left(\tfrac{\varepsilon}{3.71}\right)\right)^{-2} \end{aligned}\right\} \tag{11}$$

3.8. Symbolic Regression-Based Unified Equation

Using the same idea as used to develop an explicit approximation of the Colebrook equation through symbolic regression [47], which is further developed in [32,33], here gives two completely new unified formulas; Equations (12) and (13):

$$\lambda \approx 0.024202 + \varepsilon + \frac{50.701}{Re} - \frac{254760 + 16876000\cdot\varepsilon}{13838000 + Re^2} \tag{12}$$

$$\lambda \approx \frac{61.395}{Re} + \frac{0.024444 + 0.60915\cdot\varepsilon}{e^{\left(\frac{8188400}{Re^2}\right)}} \tag{13}$$

The symbolic model was found by Eureqa Newtonian software [48,49]. The approximation is very computationally efficient, as it requires only basic arithmetic operations. Only elementary operations (+, −, ×, /) were used in Eureqa as building blocks of the symbolic regression process. Consequently, Equation (12) obtained is a simple, rational function following reasoning as in Praks and Brkić [50]. Contrary to Equation (12), the exponential function was also allowed as the building block in Eureqa, which gives Equation (13). The advantage of Equation (13) is that the approximation is very simple and explainable, where, e.g., the first part 61.395/Re corresponds to laminar flow.

Equations (12) and (13) were obtained by the following three steps:

1. Quasi Monte Carlo sampling [51,52] of Equation (5) from Section 3.1 of this Communication was constructed to obtain a table of triplets with n = 65,535 combinations of the Reynolds number Re, the relative roughness of inner pipe surface ε and Darcy's flow friction λ according to Praks and Brkić [53]; then,
2. the symbolic regression tool Eureqa [48,49] was used to build the explicit approximation of Darcy's flow friction λ using the obtained triplets from the previous step, and finally

3. constants of Equation (12) were optimized in Matlab using the derivative-free method "fminsearch" [54] to minimize the absolute value of the relative error of the approximation.

To develop Equations (12) and (13) from this section, experience gained from developing the Artificial Neural Network for modelling hydraulic resistance was valuable [55].

None of the already existed formulations cannot be accepted as accurate, but, for the purpose of comparisons, Equation (5) is considered the ground truth for the error analysis to feed the accurate value λ_i, while $\overline{\lambda}_i$ is taken from λ calculated using Equations (12) and (13) to calculate the Mean Absolute Error (MAE); $MAE = \frac{1}{n}\sum_{i=1}^{n}\left|\lambda_i - \overline{\lambda}_i\right|$ is in a sufficient number of testing points $i = 1, 2, \ldots, n$ where the symbol n represents the number of combinations of the Reynolds number Re, the relative roughness of the inner pipe surface ε and Darcy's flow friction λ; n = 65,535 in this case. The Mean Absolute Error (MAE) for Equation (12) is 0.004673045, and, for Equation (13), it is 0.000281439.

4. Graphical Interpretation and Discussion

No matter which formula is used for the eight presented, the general trend is the same as can be seen in Figure 2. The comparison of the presented formulas shows relative variation among them due to differences in their nature; some of them follow Colebrook's formula while some follow Nikuradse's findings as listed in Table 1. In addition, Table 1 shows which of the presented formulations are flexible, i.e., which can be modified using different available formulations for turbulent flow (interchangeable).

Using the presented equations, Darcy's friction factor λ can be easily calculated no matter which type of hydraulic flow, laminar or turbulent, occurs in the observed pipeline. The main strength of the presented formulations is that, with the known values of input parameters, the Reynolds number Re and the relative roughness of inner pipe surface ε, it is not required to know in advance if laminar or turbulent types of flow occur in the observed pipeline.

A new formulation based on symbolic regression presented in this paper as Equation (12) or Equation (13), relatively well fitting all already available formulations for the same purpose.

The real evaluation of the presented formulations is not easy to perform because, although universally accepted as an informal standard, it is questionable how accurate the Colebrook equation is, or how reliable data from Nikuradse's experiment are knowing that his data were measured on very rough pipes, compared to modern materials and that they are a little old, and there is also the controversy with unreported corrections he made to the data [56–62]. In the final instance, the only valuable comparison can come through real measurements, which are relatively rare [63,64].

In addition, last but not least, it is not easy to estimate with sufficient accuracy the value of the relative roughness of the inner pipe surface ε [65–67].

Table 1. Formulations that follow monotonic [1] and inflectional [2] shape of curves in turbulent flow and ability for modification.

Formulation	Type	Flexible [3]
Equation (5)	Inflectional	Partially
Equation (6)	Monotonic	Yes
Equation (7)	Monotonic	Yes
Equation (8)	Monotonic	No
Equation (9)	Inflectional	Partially
Equation (10)	Monotonic	Partially
Equation (11)	Inflectional	Yes
Equation (12)	Inflectional	No
Equation (13)	Inflectional	No

[1] Colebrook type, [2] Nikuradse type, [3] Can it be modified using other different equations?

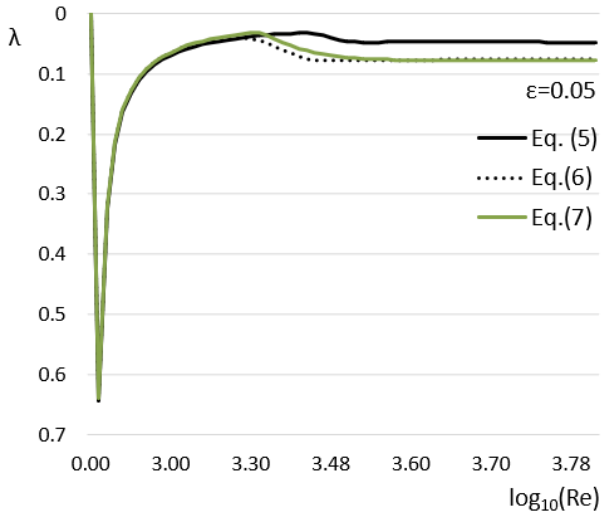

(**a**)

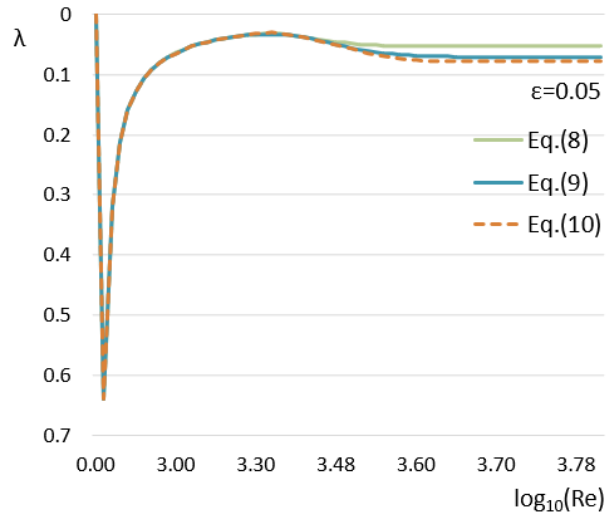

(**b**)

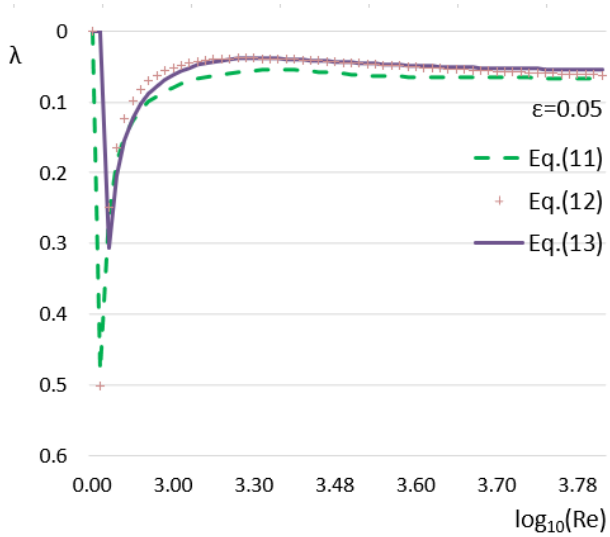

(**c**)

Figure 2. Graphical interpretation of all eight presented equations: (**a**) Equations (5)–(7); (**b**) Equations (8)–(10); and (**c**) Equations (11)–(13).

5. Conclusions

In addition to a short overview of already existing models that unifies laminar and turbulent formulations of flow friction, two new formulations based on symbolic regression are given. Compared with the other seven models, the new approximations are relatively simple. None of those shown existed already, and the new ones cannot be favorized as the more accurate because all of them were developed using different experimental approaches. The submarine model was developed initially for offshore pipelines, whereas the Churchill equation, the Russian formula for transport of crude oil, and the two new symbolic regression-based unified equations are relatively simple. On the other hand, the Multisegmented equation and the unified model based on the turbulent transitional formula are flexible because they can be easily readapted using different experimental formulas from the available literature. By definition, the Six parameter model, Interpolation method and Multisegmented method always follow behaviour from Nikuradse's experiment, while the new symbolic regression-based unified equations are also based on the Six parameter model, resulting in it being the only available relatively simple formulation that follows the behaviour of flow predicted by Nikuradse.

Based on the analysis from this Communication, every presented equation can be used in engineering practice while the final decision can be made based on simplicity and on the experimental data, which is preferred based on the previous experience of the designer. A weak point of the two new formulas is that regression was based on other formulae and not on actual experimental data (because of that error, all equations have very limited application and are only illustrative).

Supplementary Materials: The following supporting information can be downloaded at: https://www.mdpi.com/article/10.3390/axioms11050198/s1. The software tool for testing all presented equations is written in Python and given as attached materials.

Author Contributions: Conceptualization, M.M. and D.B.; methodology, D.B.; software, M.M., D.B. and P.P.; validation, D.L. and Z.S.; error analysis, P.P. and D.B.; formal analysis, D.B.; investigation, M.M.; resources, D.B.; data curation, D.B. and D.L.; writing—original draft preparation, D.B.; writing—review and editing, M.M., D.B. and P.P.; visualization, D.B.; supervision, Z.S.; project administration, D.B.; funding acquisition, D.B. and Z.S. All authors have read and agreed to the published version of the manuscript.

Funding: This work has been supported by the Ministry of Education, Science and Technological Development of the Republic of Serbia and by the Technology Agency of the Czech Republic through the project CEET—"Center of Energy and Environmental Technologies" TK03020027.

Data Availability Statement: All data to repeat computations are given in the text.

Conflicts of Interest: The authors declare no conflict of interest.

References

1. Altowayti, W.A.H.; Othman, N.; Tajarudin, H.A.; Al-Dhaqm, A.; Asharuddin, S.M.; Al-Gheethi, A.; Alshalif, A.F.; Salem, A.A.; Din, M.F.M.; Fitriani, N.; et al. Evaluating the Pressure and Loss Behavior in Water Pipes Using Smart Mathematical Modelling. *Water* **2021**, *13*, 3500. [CrossRef]
2. Kraszewska, A.; Donizak, J. An Analysis of a Laminar-Turbulent Transition and Thermal Plumes Behavior in a Paramagnetic Fluid Subjected to an External Magnetic Field. *Energies* **2021**, *14*, 7972. [CrossRef]
3. Brkić, D.; Praks, P. Air-Forced Flow in Proton Exchange Membrane Fuel Cells: Calculation of Fan-Induced Friction in Open-Cathode Conduits with Virtual Roughness. *Processes* **2020**, *8*, 686. [CrossRef]
4. Billard, L.; Diday, E. Symbolic Regression Analysis. In *Classification, Clustering, and Data Analysis. Studies in Classification, Data Analysis, and Knowledge Organization*; Jajuga, K., Sokołowski, A., Bock, H.H., Eds.; Springer: Berlin/Heidelberg, Germany, 2002. [CrossRef]
5. Swamee, P.K. Design of a submarine oil pipeline. *J. Transp. Eng.* **1993**, *119*, 159–170. [CrossRef]
6. Submarine Pipeline Systems. Offshore Standard DNV-OS-F101 by Det Norske Veritas AS, Edition 2021–08-Amended 2021–12. Available online: https://www.dnv.com/oilgas/download/dnv-st-f101-submarine-pipeline-systems.html (accessed on 21 February 2022).

7. Hapanowicz, J. Two-Phase Liquid–Liquid Flow in the Aspect of Reduction of Pumping Power of Hydrophobic Substances with High Viscosity. *Energies* **2021**, *14*, 2432. [CrossRef]
8. Ferro, V.; Nicosia, A. Evaluating the Effects of Sediment Transport on Pipe Flow Resistance. *Water* **2021**, *13*, 2091. [CrossRef]
9. Brown, G.O. Environmental and Water Resources History Sessions. In Proceedings of the ASCE Civil Engineering Conference and Exposition 2002, Washington, DC, USA, 3–7 November 2002; pp. 34–43. [CrossRef]
10. Brown, G.O. Henry Darcy and the making of a law. *Water Resour. Res.* **2002**, *38*, 11. [CrossRef]
11. Colebrook, C.F. Turbulent flow in pipes with particular reference to the transition region between the smooth and rough pipe laws. *J. Inst. Civ. Eng.* **1939**, *11*, 133–156. [CrossRef]
12. Colebrook, C.F.; White, C.M. Experiments with fluid friction in roughened pipes. *Proc. R. Soc. London. Ser. A-Math. Phys. Sci.* **1937**, *161*, 367–381. [CrossRef]
13. Nikuradse, J. Laws of Flow in Rough Pipes (Strömungsgesetze in Rauhen Rohren). Available online: https://ntrs.nasa.gov/citations/19930093938 (accessed on 21 February 2022).
14. Thakkar, M.; Busse, A.; Sandham, N.D. Direct numerical simulation of turbulent channel flow over a surrogate for Nikuradse-type roughness. *J. Fluid Mech.* **2018**, *837*, R1. [CrossRef]
15. McKeon, B.J.; Swanson, C.J.; Zagarola, M.V.; Donnelly, R.J.; Smits, A.J. Friction factors for smooth pipe flow. *J. Fluid Mech.* **2004**, *511*, 41–44. [CrossRef]
16. Eck, B.J. Use of a smoothed model for pipe friction loss. *J. Hydraul. Eng.* **2017**, *143*, 06016022. [CrossRef]
17. Basse, N.T. Turbulence Intensity and the Friction Factor for Smooth- and Rough-Wall Pipe Flow. *Fluids* **2017**, *2*, 30. [CrossRef]
18. Rocha, H.S.D.; Marques, P.A.; Camargo, A.P.D.; Frizzone, J.A.; Saretta, E. Internal surface roughness of plastic pipes for irrigation. *Rev. Bras. Eng. Agríc. Ambient.* **2017**, *21*, 143–149. [CrossRef]
19. Da Silva, J.G.; Peiter, M.X.; Robaina, A.D.; Bruning, J.; Neto, M.C.; Ferreira, L.D. Simplified Scobey formula for determining head loss in pressurized pipes. *Rev. Bras. Agric. Irrig. RBAI* **2022**, *16*, 31–41. [CrossRef]
20. Ullah, A.M.M.S. Surface Roughness Modeling Using Q-Sequence. *Math. Comput. Appl.* **2017**, *22*, 33. [CrossRef]
21. Santos-Ruiz, I.; López-Estrada, F.-R.; Puig, V.; Valencia-Palomo, G. Simultaneous Optimal Estimation of Roughness and Minor Loss Coefficients in a Pipeline. *Math. Comput. Appl.* **2020**, *25*, 56. [CrossRef]
22. Brkić, D. Can pipes be actually really that smooth? *Int. J. Refrig.* **2012**, *35*, 209–215. [CrossRef]
23. Moody, L.F. Friction factors for pipe flow. *Trans. ASME* **1944**, *66*, 671–684.
24. LaViolette, M. On the history, science, and technology included in the Moody diagram. *J. Fluids Eng.* **2017**, *139*, 030801. [CrossRef]
25. Madeira, A.A. Major and minor head losses in a hydraulic flow circuit: Experimental measurements and a Moody's diagram application. *Eclética Quím.* **2020**, *45*, 47–56. [CrossRef]
26. McGovern, J. Friction Factor Diagrams for Pipe Flow. 2011. Available online: https://arrow.dit.ie/engschmecart/28/ (accessed on 21 February 2022).
27. Abdolahi, F.; Mesbah, A.; Boozarjomehry, R.B.; Svrcek, W.Y. The effect of major parameters on simulation results of gas pipelines. *Int. J. Mech. Sci.* **2007**, *49*, 989–1000. [CrossRef]
28. Díaz-Damacillo, L.; Plascencia, G. A new six parameter model to estimate the friction factor. *AIChE J.* **2019**, *65*, 1144–1148. [CrossRef]
29. Plascencia, G.; Díaz–Damacillo, L.; Robles-Agudo, M. On the estimation of the friction factor: A review of recent approaches. *SN Appl. Sci.* **2020**, *2*, 1–13. [CrossRef]
30. Avci, A.; Karagoz, I. A new explicit friction factor formula for laminar, transition and turbulent flows in smooth and rough pipes. *Eur. J. Mech. B Fluids* **2019**, *78*, 182–187. [CrossRef]
31. Avci, A.; Karagoz, I. A novel explicit equation for friction factor in smooth and rough pipes. *J. Fluids Eng.* **2009**, *131*, 061203. [CrossRef]
32. Praks, P.; Brkić, D. Review of new flow friction equations: Constructing Colebrook explicit correlations accurately. *Rev. Int. Métodos Numér. Cálc. Diseño Ing.* **2020**, *36*, 41. [CrossRef]
33. Brkić, D.; Praks, P. Accurate and Efficient Explicit Approximations of the Colebrook Flow Friction Equation Based on the Wright ω-Function. *Mathematics* **2019**, *7*, 34. [CrossRef]
34. Brkić, D. Review of explicit approximations to the Colebrook relation for flow friction. *J. Pet. Sci. Eng.* **2011**, *77*, 34–48. [CrossRef]
35. Brkić, D.; Stajić, Z. Excel VBA-based user defined functions for highly precise Colebrook's pipe flow friction approximations: A Comparative overview. *Facta Univ. Ser. Mech. Eng.* **2021**, *19*, 7267. [CrossRef]
36. Zeyu, Z.; Junrui, C.; Zhanbin, L.; Zengguang, X.; Peng, L. Approximations of the Darcy–Weisbach friction factor in a vertical pipe with full flow regime. *Water Supply* **2020**, *20*, 1321–1333. [CrossRef]
37. Naseri, A.; Nikazar, M.; Dehghani, S.M. A correlation approach for prediction of crude oil viscosities. *J. Pet. Sci. Eng.* **2005**, *47*, 163–174. [CrossRef]
38. Brkić, D. Discussion of "Economics and statistical evaluations of using Microsoft Excel solver in pipe network analysis". *J. Pipeline Syst. Eng. Pract.* **2018**, *9*, 07018002. [CrossRef]
39. Swamee, P.K.; Jain, A.K. Explicit equations for pipe-flow problems. *J. Hydraul. Div.* **1976**, *102*, 657–664. [CrossRef]
40. Черникин, В.А.; Черникин, А.В. Обобщенная формула для расчета коэффициента гидравлического сопротивления магистральных трубопроводов для светлых нефтепродуктов и маловязких нефтей. *Наука И Технологии Трубопроводного*

Транспорта Нефти И Нефтепродуктов **2012**, *4*, 64–66. Available online: http://transenergostroy.ru/publications/src/20130424/Chernikin_gidrav_soprotivlenie.pdf (accessed on 22 February 2022). (In Russian).
41. Альтшуль, А.Д. *Гидравлические Сопротивления*; Недра: Moscow, Russia, 1982. (In Russian)
42. Cheng, N.S. Formulas for friction factor in transitional regimes. *J. Hydraul. Eng.* **2008**, *134*, 1357–1362. [CrossRef]
43. Churchill, S.W. Friction-factor equation spans all fluid-flow regimes. *Chem. Eng.* **1977**, *84*, 91–92.
44. Churchill, S.W. Empirical expressions for the shear stress in turbulent flow in commercial pipe. *AIChE J.* **1973**, *19*, 375–376. [CrossRef]
45. Brkić, D.; Praks, P. Unified friction formulation from laminar to fully rough turbulent flow. *Appl. Sci.* **2018**, *8*, 2036. [CrossRef]
46. Uršič, M.; Kompare, B. Improvement of the hydraulic friction losses equations for flow under pressure in circular pipes. *Acta Hydrotech.* **2003**, *21*, 57–74. Available online: https://actahydrotechnica.fgg.uni-lj.si/en/paper/a34mu (accessed on 22 February 2022).
47. Praks, P.; Brkić, D. Symbolic regression-based genetic approximations of the Colebrook equation for flow friction. *Water* **2018**, *10*, 1175. [CrossRef]
48. Dubčáková, R. Eureqa: Software review. *Genet. Program. Evol. Mach.* **2011**, *12*, 173–178. [CrossRef]
49. Stoutemyer, D.R. Can the Eureqa symbolic regression program, computer algebra and numerical analysis help each other. *Not. AMS* **2003**, *60*, 713–724. [CrossRef]
50. Praks, P.; Brkić, D. Rational approximation for solving an implicitly given Colebrook flow friction equation. *Mathematics* **2020**, *8*, 26. [CrossRef]
51. Askar, T.; Shukirgaliyev, B.; Lukac, M.; Abdikamalov, E. Evaluation of Pseudo-Random Number Generation on GPU Cards. *Computation* **2021**, *9*, 142. [CrossRef]
52. Cordero, A.; Martí, P.; Victoria, M. Optimización de topología robusta de estructuras continuas usando el método de Monte Carlo y modelos Kriging (Robust topology optimization of continuum structures using Monte Carlo method and Kriging models). *Rev. Int. Métodos Numér. Cálc. Diseño Ing.* **2018**, *34*, 5. (In Spanish) [CrossRef]
53. Praks, P.; Brkić, D. Approximate flow friction factor: Estimation of the accuracy using Sobol's quasi-random sampling. *Axioms* **2022**, *11*, 36. [CrossRef]
54. Liu, H.; Huang, J.; Guan, Y.; Sun, L. Accelerated Degradation Model of Nonlinear Wiener Process Based on Fixed Time Index. *Mathematics* **2019**, *7*, 416. [CrossRef]
55. Srivastava, V.; Prakash, A.; Rawat, A. To Predict Frictional Pressure-Drop of Turbulent Flow of Water Through a Uniform Cross-Section Pipe Using an Artificial Neural Network. In *Recent Advances in Applied Mechanics*; Springer: Singapore, 2022; pp. 397–412. [CrossRef]
56. Brownlie, W.R. Re-examination of Nikuradse roughness data. *J. Hydraul. Div.* **1981**, *107*, 115–119. [CrossRef]
57. Beattie, D.R.H. In Defence of Nikuradse. In Proceedings of the Twelfth Australasian Fluid Mechanics Conference, The University of Sydney, Sydney, Australia, 10–15 December 1995. Available online: https://people.eng.unimelb.edu.au/imarusic/proceedings/12/Beattie.pdf (accessed on 22 February 2022).
58. Hager, W.H.; Liiv, U. Johann Nikuradse–hydraulic experimenter. *J. Hydraul. Res.* **2008**, *46*, 435–444. [CrossRef]
59. Yang, B.H.; Joseph, D.D. Virtual Nikuradse. *J. Turbul.* **2009**, *10*, N11. [CrossRef]
60. Joseph, D.D.; Yang, B.H. Friction factor correlations for laminar, transition and turbulent flow in smooth pipes. *Phys. D Nonlinear Phenom.* **2010**, *239*, 1318–1328. [CrossRef]
61. Choe, Y.-W.; Sim, S.-B.; Choo, Y.-M. New equation for predicting pipe friction coefficients using the statistical based entropy concepts. *Entropy* **2021**, *23*, 611. [CrossRef]
62. Qiu, M.; Ostfeld, A. A head formulation for the steady-state analysis of water distribution systems using an explicit and exact expression of the Colebrook–White equation. *Water* **2021**, *13*, 1163. [CrossRef]
63. Österlund, J.M.; Johansson, A.V.; Nagib, H.M.; Hites, M.H. A note on the overlap region in turbulent boundary layers. *Phys. Fluids* **2000**, *12*, 1–4. [CrossRef]
64. Perry, A.E.; Hafez, S.; Chong, M.S. A possible reinterpretation of the Princeton superpipe data. *J. Fluid Mech.* **2001**, *439*, 395–401. [CrossRef]
65. Muzzo, L.E.; Matoba, G.K.; Ribeiro, L.F. Uncertainty of pipe flow friction factor equations. *Mech. Res. Commun.* **2021**, *116*, 103764. [CrossRef]
66. Zmrhal, V.; Boháč, J. Pressure loss of flexible ventilation ducts for residential ventilation: Absolute roughness and compression effect. *J. Build. Eng.* **2021**, *44*, 103320. [CrossRef]
67. Pimenta, B.D.; Robaina, A.D.; Peiter, M.X.; da Rocha, H.S.; Sobenko, L.R.; da Conceição, C.G. Use of bench and portable rugosimeters in evaluatingthe internal roughness of PVC pipes of different diameters. *Rev. Bras. Ciências Agrárias* **2022**, *17*, 1–7. [CrossRef]